RESEARCH ARTICLE

Editor's Choice

ADVANCED MATERIALS TECHNOLOGIES

www.advmattechnol.de

# Self-Destructible Electromagnetic Interference Shielding Films

*Yang Zhou, Yamin Pan,* Chuntai Liu, Changyu Shen, and Xianhu Liu**

**In response to the increasing utilization of communication technology, there is a growing need for electromagnetic interference (EMI) shielding materials to adapt to diverse application scenarios. In this study, the self-destructible EMI shielding films (SEFs) that possess the unique capability to reduce conductivity and shielding efficiency through temperature elevation are introduced. The SEFs effectively fulfill the requirement of triggering EMI shielding failure under specific conditions, which can be achieved by simply spraying a mixture of thermally expandable microspheres (TEMs), conductive fillers, and resin substrates. The segregated structures resulting from the incorporation of TEMs confer exceptional electrical conductivity and superior EMI shielding performance at low conductive filler content. When the ambient temperature surpasses the glass transition temperature of the TEM shell, the thermally expandable characteristics cause a disruption in the conductive path of the SEFs, leading to a significant decline in shielding effectiveness. Additionally, the SEFs exhibit outstanding Joule heating effects (90 °C) at low voltage (1.5 V) within a brief time frame (10 s). Importantly, when employed as Joule heaters, the SEFs possess an intrinsic safety mechanism that automatically ceases operation in the event of circuit overload, thus minimizing any potential risks.**

## 1. Introduction

In the new millennium, humanity has set its sights on two ambitious objectives: the resurgence of lunar exploration and the achievement of a manned expedition to Mars. The intricate electromagnetic conditions prevailing in space necessitate the incorporation of highly efficient electromagnetic interference (EMI) shielding materials within spacecraft. Nevertheless, in the event of inadvertent damage to the external communication equipment, astronauts may find themselves compelled to rely on portable communication devices within the confines of their spacecraft for emergency purposes. To better achieve this objective, it is advisable to utilize self-destructible EMI shielding materials. Conductive polymer composites (CPCs), which consist of conductive fillers and polymer matrix, offer several advantages over traditional metal shielding materials. These advantages include lightweight, high flexibility, and corrosion resistance, making CPCs a more suitable option for the development of self-destructible EMI shielding materials, when used in the aeronautical materials.[1-15]

Thermally expandable microspheres (TEMs) are polymeric particles consisting of thermoplastic polymer shell and low-boiling alkane liquid. Once the temperature surpasses the glass transition temperature of the shell, the shell undergoes softening and subsequently expands. As a result of internal pressure, the volume can increase to 50–100 times larger than its original size. When the temperature drops to room temperature, the shell returns to its glassy state and retains its expanded size. This unique behavior imparts self-destructible EMI shielding ability to the CPCs materials.[16–19] In recent years, utilizing TEMs to prepare CPCs has garnered significant interest from the scholarly community.[20–27] Cai et al. obtained the tunable EMI shielding in polydimethylsiloxane (PMDS)/TEMs/carbon nanotube (CNT) composites. EMI shielding effect of the composites could be modifiable by manipulating the temperature and compression strain.[23] The TEMs were also used to construct segregated structures in CPCs to enhance the electrical conductivity and EMI shielding performance.[28–37] Xue et al. incorporated TEMs into CNT/Ecoflex composite to develop a flexible strain sensor with enhanced sensitivity. The presence of TEMs in the composite significantly enhanced the conductivity of the conductive polymers.[18] This suggests that TEMs are promising candidates for the construction of thermally responsive conductive polymers, as they can effectively improve the

Y. Zhou, Y. Pan
College of Material Science and Engineering
Zhengzhou University
Zhengzhou 450001, China
E-mail: yamin.pan@zzu.edu.cn

Y. Zhou, C. Liu, C. Shen, X. Liu
National Engineering Research Center for Advanced Polymer Processing Technology
Zhengzhou University
Zhengzhou 450002, China
E-mail: xianhu.liu@zzu.edu.cn

The ORCID identification number(s) for the author(s) of this article can be found under https://doi.org/10.1002/admt.202302026

DOI: 10.1002/admt.202302026

 

conductivity by volume exclusion effect. Overall, most of the literatures use TEMs to enhance the conductivity or EMI shielding efficiency, but few literatures use TEMs to prepare self-destructible EMI shielding films.

Herein, self-destructible EMI shielding films (SEFs) with segregated structure was prepared based on TEMs. Comparing with the homogeneous films, the films with segregated structures demonstrate significantly improved conductivity and EMI shielding capabilities, primarily due to the presence of TEMs creating an excluded volume. The inclusion of TEMs in the films also imparts them with self-destructible EMI shielding performance, thanks to their thermally expandable properties. Meanwhile, TEMs endow the films a huge potential application for overheating protection when they act as Joule heaters. Furthermore, the composite films can also monitor abnormal high temperature in real time and promptly emit alarm signals.

## 2. Result and Discussion

### 2.1. Mechanism and Design

The mechanism of SEFs using TEMs is visually depicted in **Figure 1**. TEMs are composed of thermoplastic resin shells and liquid hydrocarbon inside. Upon exposure to temperatures beyond the shell's glass transition temperature, the shell softens and the liquid hydrocarbon inside boils to push the shell into expansion (Figure 1a). Figure 1b shows the TEMs in their initial state and expansion state after heating at 125 °C. Notably, a significant increase in volume is observed. As depicted in Figure 1c, the TEMs are incorporated into the film, forming a 3D segregate structure together with conductive fillers. This integration serves to improve the conductivity of the film, while reducing its overall density.[29–30] Then, TEMs undergo expansion when the temperature surpasses a predetermined threshold, leading to an increased separation between conductive fillers. Consequently, this phenomenon disrupts the initial conductive pathway of the films. As a result, the SEFs showcase an ability to regulate the self-destructible EMI shielding performance through the utilization of TEMs.

To further understand the self-destructible behavior of the SEFs, the waterborne polyurethane is used as matrix and the typical examples for their cross-section diagrams are given. Pure polymer films exhibit smooth surface (Figure S2, Supporting Information), whereas conductive fillers are evenly dispersed, forming "brick-mud" structures within the films (Figure 1d). After the TEMs are further introduced (Figure 1e), the conductive fillers are distributed among the TEMs. The excluded volume effect caused by TEMs leads to a closer arrangement of conductive fillers, transforming the "brick-mud" structures into segregated structures within the films. This rearrangement directly impacts the electrical conductivity and EMI shielding performance of the films. When the film is subjected to heat at 125 °C for 30 min, the TEMs expand, increasing the distance between the conductive fillers. The cross-section of the heated film is illustrated in Figure 1f, demonstrating the self-destructible properties of the SEFs and their potential application in the field of overheating protection.

In addition, a possible application scenario of the SEFs as a lightweight EMI shielding material for manned spacecraft is shown in Figure 1g. In typical conditions, the SEFs possess notable electrical conductivity and effectively shield electromagnetic waves. When the spacecraft's communication equipment is accidentally broken, the self-destructible function could be activated to allow electromagnetic waves passing through the film. At this point, the astronauts could communicate through the equipment in the cabin.

### 2.2. EMI Shielding and Self-Destructible Performance

To further understand the SEFs performance, herein the silver-coated copper powders as the conductive fillers are chosen, and the prepared films are named SEFs-x/y, where "x" and "y" represent the mass fraction of conductive fillers and TEMs, respectively. As shown in **Figure 2**a, the conductivity of the films experiences a notable enhancement as the content of TEMs increases. This improvement can be attributed to the creation of an excluded volume by TEMs, leading to the formation of a segregated conductive network among conductive fillers.[25,29] No matter what the content of conductive filler is, the increase in TEMs content in the SEFs leads to an apparent enhancement in the EMI SE (Figure 2b and Figure S3, Supporting Information). However, it should be noted that when the conductive fillers content in the SEFs remains constant, the conductivity and EMI SE cannot be improved indefinitely by adding TEMs. The EMI SE of the SEFs-40/0 is measured to be 41 dB. In contrast, the EMI SE of the SEFs-40/15 increases to 65 dB as the TEMs content goes from 0 to 15 wt.%. Furthermore, when the TEMs content further increases from 15 to 25 wt.%, the EMI SE shows a slight improvement from 65 to 71 dB. Notably, the SEFs-50/15 exhibits a significantly high EMI SE of 90.1 dB, while the SEFs-50/0 only achieves a value of 61.8 dB (Figure S3, Supporting Information).

The $SE_R$ and $SE_A$ of the SEFs containing 40 wt.% conductive fillers are displayed in Figure 2c. The inclusion of TEMs in the samples resulted in a gradual enhancement of both $SE_A$ and $SE_T$. This observation implies that the films exhibit an increased ability to absorb electromagnetic waves that permeate through the film.[28] Meanwhile, the relative size of $SE_R$ and $SE_A$ cannot determine whether the composite films can be classified as absorption-dominated shielding materials. The reflection coefficient (R), absorption coefficient (A), and transmission coefficient (T) were calculated and shown in Figure 2d. The value of R for a series of films is higher than the value of A, suggesting that the primary shielding mechanism of the composite films is reflection.[38]

The mechanical properties of the SEFs are crucial for practical application. The stress-strain curves, elongation at break and tensile strength of the SEFs are placed in Figure S6 (Supporting Information). The conductive filler content in the SEFs was fixed at 40 wt.%, and then we further added TEMs into the SEFs to analyze changes in mechanical properties. With the increase of TEMs content, the elongation at break of the SEFs decreases from 409% of the SEFs-40/0 to 56% of the SEFs-40/25. The tensile strength also decreases with the increase of TEMs. These behaviors show that excessive fillers will degrade the mechanical properties of the SEFs, which is significant for the preparation of SEFs in the practical application.

The temperature-induced self-destructible behavior of the films was observed in the experiment. Figure 2e depicts the

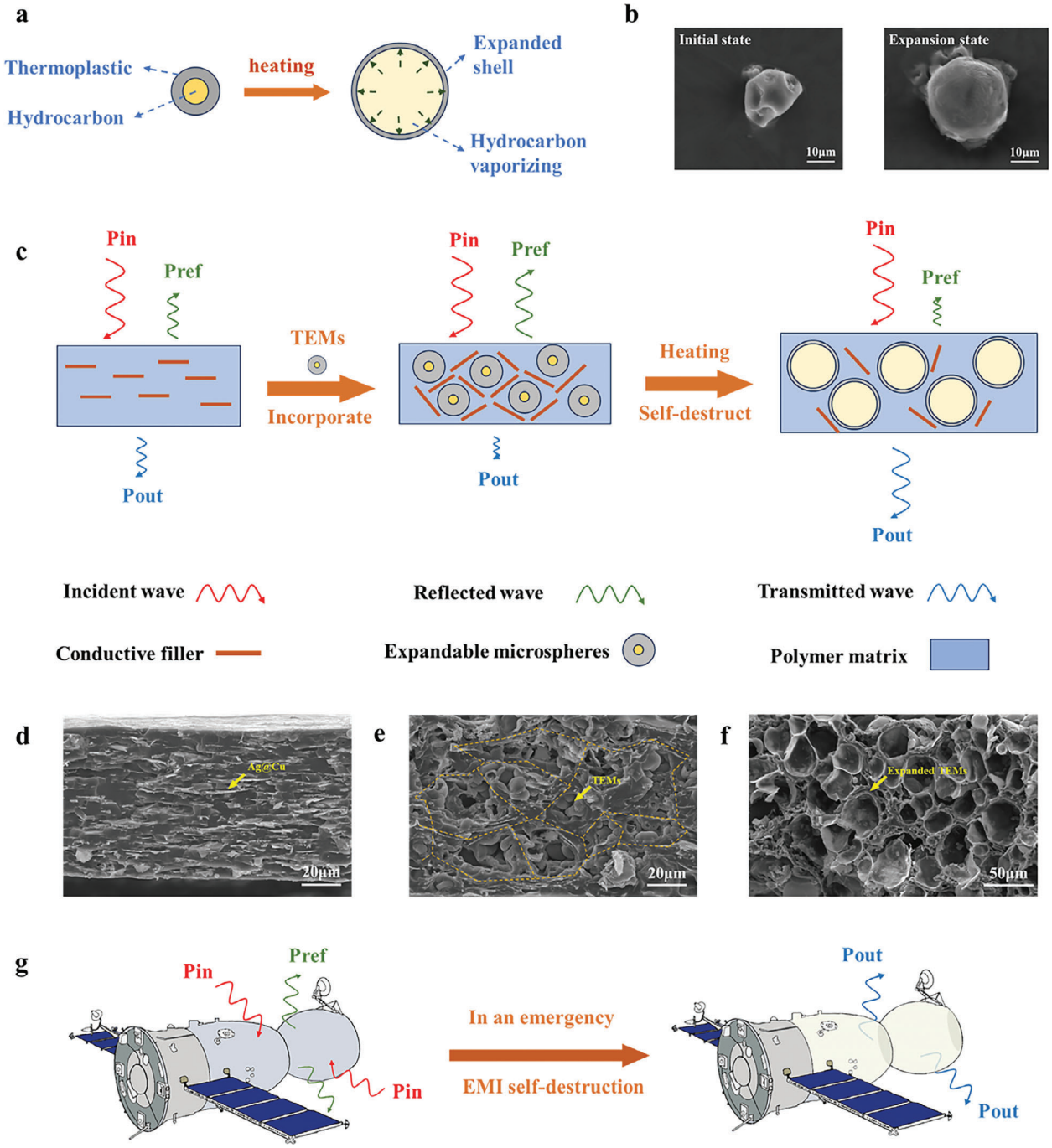


**Figure 1.** Preparation, mechanism, and application of self-destructible EMI shielding films (SEFs). a) Schematic illustration of the expansion mechanism of TEMs. b) SEM images of TEMs before (Initial state) and after (Expansion state) being heated. c) The mechanism of the self-destructible performance. Cross-sectional SEM images of d) traditional conductive films, e, f) SEFs before e) and f) after heating. g) Possible application scenario of the SEFs as an EMI shielding material for manned spacecraft.

decreasing conductivity of SEFs-40/15 as the heating time in an oven at 125 °C is prolonged. This can be attributed to the destruction of the conductive path by the expanded TEMs. The EMI SE of the films decreases continuously with the extension of heating time as shown in Figure 2f. This phenomenon can be explained by two factors. On the one hand, the impedance mismatch is weakened due to the decrease of resistance; and on the other hand, the gaps between conductive fillers increase, resulting in the electromagnetic wave transmitting out of the films instead of being absorbed by multiple reflections. Therefore, the $SE_R$ and $SE_A$ of SEFs-40/15 will also decrease with the extension of heating time (Figure S5, Supporting Information).

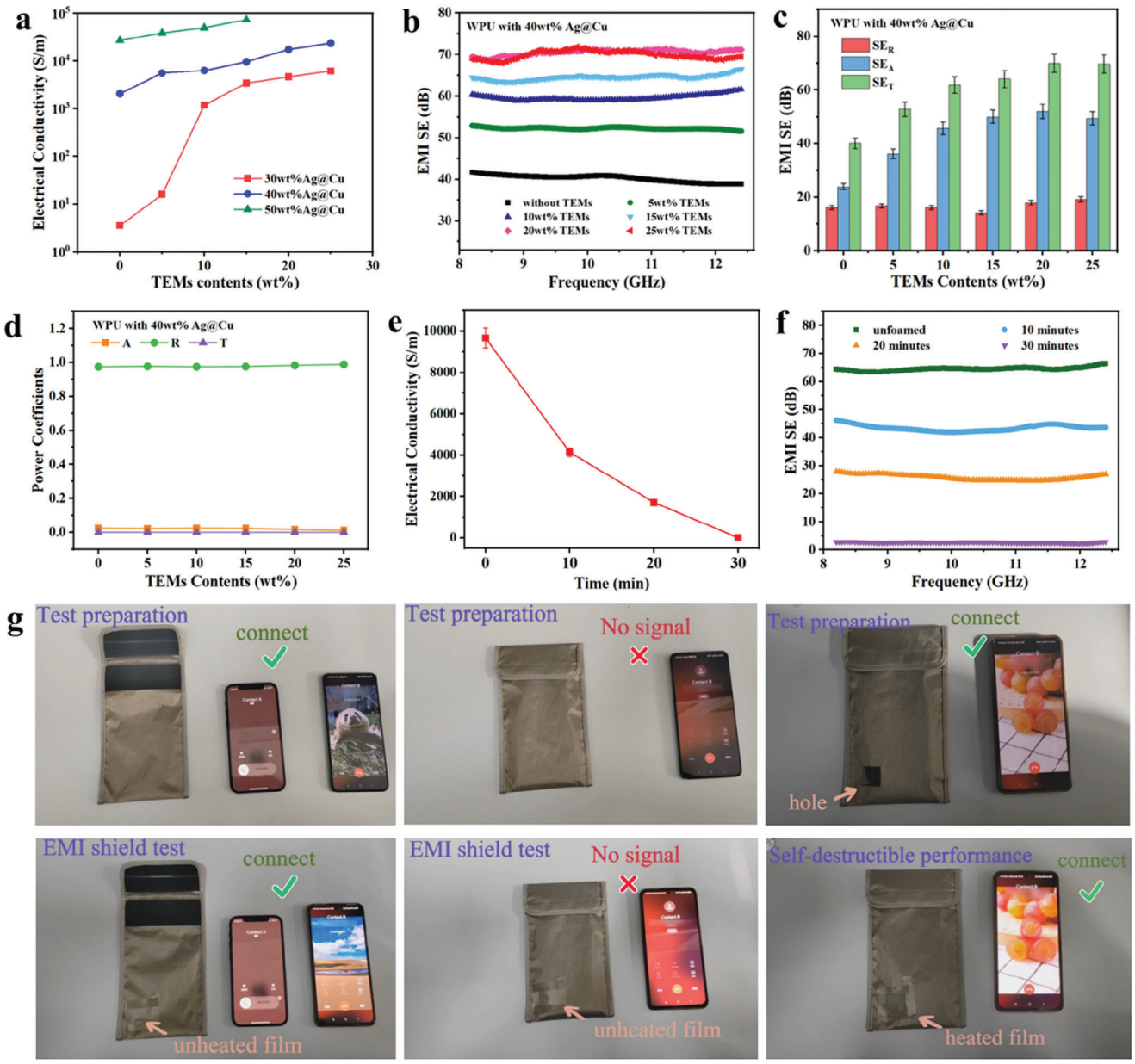


**Figure 2.** The change in EMI performance of the SEFs. a) Electrical conductivity of the SEFs, b) EMI SE. c) $SE_R$, $SE_A$, d) Average power coefficients of A, R, and T of SEFs with 40 wt.% conductive fillers and different TEMs contents. e) Electrical conductivity, f) EMI SE of the SEFs-40/15 heated for 0, 10, 20, and 30 min at 125 °C. g) A real self-destructible EMI application measurement in mobile phone signal shielding bag.

The actual self-destructible EMI shielding performance of the film is also tested (Figure 2g and Video S1, Supporting Information). The experiment was facilitated by employing a commercial mobile phone shielding bag. When the phone was not placed inside the bag, it could be answered in the usual manner. However, when the phone was placed inside the bag, no signal was detected. Subsequently, a hole was created in the mobile phone shielding bag, which allowed for normal connectivity of the internal phone. To evaluate the effectiveness of the film's shielding capability, an unheated film was affixed to the hole. As a result, the phone could not establish a connection, indicating that the unheated film possessed a robust shielding ability. Conversely, when the heated film was utilized, the phone could once again be answered normally, thereby substantiating the self-destructible property of the film when subjected to heat. The composite films are sensitive to temperature, and this self-destructible behavior endows the films the potential application in fire warning, overheating protection and manned spacecraft.

Besides the EMI SE, the density and thickness serve as critical parameters for EMI shielding materials. To compare different EMI shielding materials, the thickness-specific electromagnetic shielding effectiveness (SSE/$t$) is calculated by dividing the EMI SE by the thickness and density. Figure S8 (Supporting Information) illustrates that the density of the composite

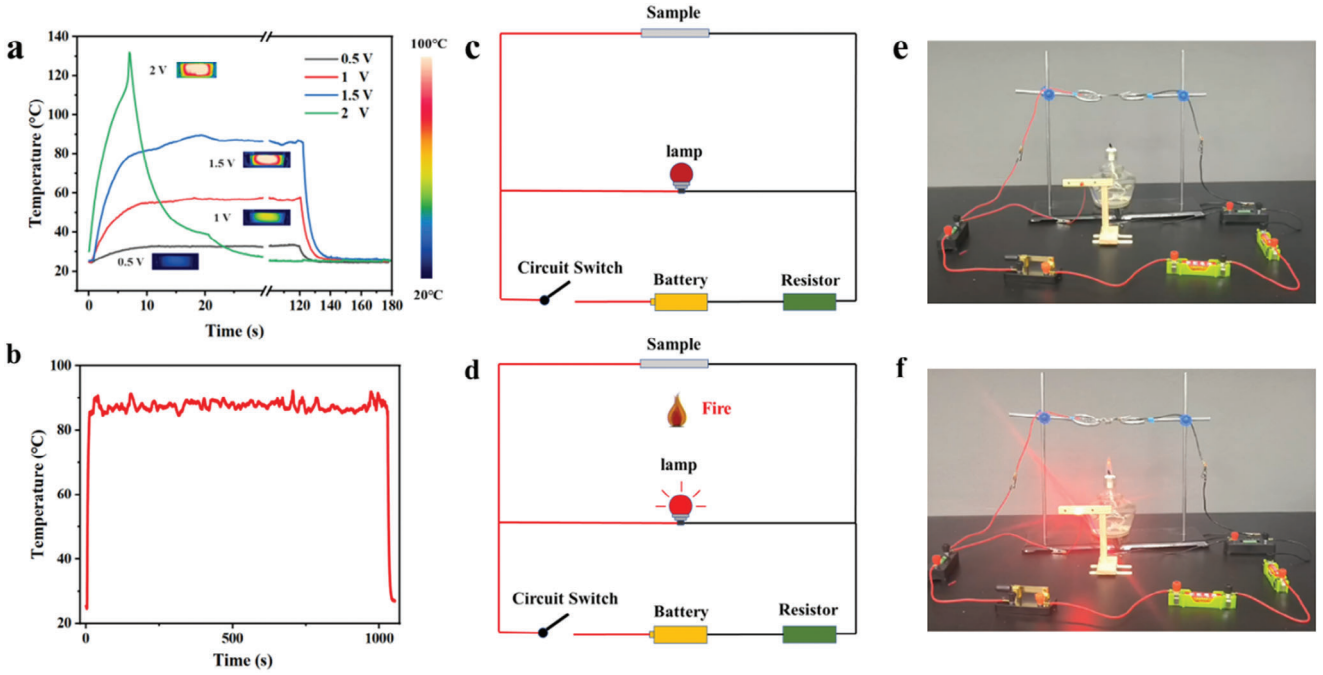


**Figure 3.** Joule heating performance and overheating protection of the SEFs-40/15. a) Temperature variation at different voltages from 0.5 to 2 V. b) Temperature stability at 1.5 V. c, d) Schematic illustration of circuit design and work mechanism of a high-temperature warning system. e, f) Digital photographs showed the high-temperature warning test process.

films decreases as the TEMs addition increases, while the SSE/$t$ value increases. This is highly significant for the preparation of lightweight EMI shielding films and their application in manned spacecraft. The EMI SE of the SEFs-50/15 is 92.9 dB, while the SSE/$t$ of these composite films reaches 8005.8 dB cm$^2$ g$^{-1}$. A comparison with other shielding materials recently reported in Figure S8c,d (Supporting Information) reveals that the EMI SE of the SEFs-50/15 is higher than most reported materials, and the SSE/$t$ of the composite films surpasses the most of metal fillers.[10,20,39–60]

### 2.3. Joule Heating Performance and Overheating Protection

In addition to the excellent EMI shielding properties, the composite films with high conductivity and thermally response behavior can also be applied as attractive Joule heaters and demonstrate immense potential in the realm of overheating protection. The surface temperature of SEFs-40/15 (4 × 1 cm$^2$) is depicted in **Figure 3**a, with an applied voltage ranging from 0.5 to 2 V. The temperature distribution is captured using an infrared camera and presented in the inserts. By adjusting the voltage from 0.5 to 1.5 V, the steady-state saturation temperature can be varied between 32–90 °C. Furthermore, a surface temperature of 90 °C can be achieved within a mere 10 seconds when the voltage is set at 1.5 V. It is essential for Joule heaters to prevent the abnormal increase in temperature when the circuit voltage is unstable. The unique surface temperature variation under the voltage of 2 V is also shown in Figure 3a. Initially, the temperature rises from ambient conditions to 125 °C, which is the glass transition temperature of the shell. At this point, the TEMs expand and disrupt the conductive network of conductive fillers. Consequently, the current passing through the films decreases, resulting in reduced heat generation. As a result, the temperature of the films rapidly decreases after reaching its peak, which shows the overheating protection ability of the films.

Furthermore, Figure S9 (Supporting Information) displays the cyclic Joule heating performance under a voltage of 1.5 V, demonstrating the films' excellent reproducibility after switching. Additionally, Figure 3b presents the measurement of the heating stability of SEFs-40/15 under the same voltage. The films' surface temperature reaches 90 °C and remains stable for a duration of 1000 s. These findings suggest that SEFs-40/15 possess a long-term Joule heating ability when their surface temperature is kept below the glass transition temperature of the shell. The composite films possess stable cycle heating performance and the ability to prevent abnormal increases in temperature, showing great application in maintaining temperature of manned spacecraft.

Besides providing protection against overheating, the composite films also possess the ability to detect abnormal high temperatures. To further investigate this property, we devised a circuit wherein the films were utilized as sensors (Figure 3c, d). Owing to the remarkable conductivity of the SEFs-40/15, the bulb light remains unilluminated when the composite film is connected to the circuit. However, upon exposure to a flame, the TEMs rapidly expand, causing the composite films to transition from being conductive to becoming insulating. Consequently, the bulb is illuminated and emits an alarm signal (Figure 3e, f and Video S2, Supporting Information). The self-destructible films can be applied in abnormal high-temperature detection and non-contact early warning of fire.

## 3. Conclusion

In this work, we propose the concept of a self-destructible composite film with outstanding EMI shielding performance, excellent Joule heating properties, and overheating protection. The film can be easily prepared through a simple spraying method. The presence of TEMs creates a volume exclusion effect, enhancing the electrical conductivity and EMI shielding capabilities of the SEFs. The volume of TEMs can be adjusted by controlling the temperature, allowing for the self-destructible behavior of the films under temperature changes. Additionally, the SEFs exhibit remarkable Joule heating performance and the ability to prevent abnormal temperature increases. These unique properties make SEFs suitable for potential applications in manned spacecraft.

## Supporting Information

Supporting Information is available from the Wiley Online Library or from the author.

## Conflict of Interest

The authors declare no conflict of interest.

## Data Availability Statement

The data that support the findings of this study are available from the corresponding author upon reasonable request.

## Keywords

Electromagnetic interference shielding, Joule heating, Overheating protection, Segregated structures

Received: November 24, 2023
Revised: December 20, 2023
Published online:

[1] Q.-F. Guan, Z.-M. Han, K.-P. Yang, H.-B. Yang, Z.-C. Ling, C.-H. Yin, S.-H. Yu, *Nano Lett.* **2021**, *21*, 2532.
[2] E. Li, Y. Pan, C. Wang, C. Liu, C. Shen, C. Pan, X. Liu, *ACS Appl. Mater. Interfaces* **2021**, *13*, 28996.
[3] J. Li, Y. Ding, N. Yu, Q. Gao, X. Fan, X. Wei, G. Zhang, Z. Ma, X. He, *Carbon* **2020**, *158*, 45.
[4] E. Li, Y. Pan, C. Wang, C. Liu, C. Shen, C. Pan, X. Liu, *Chem. Eng. J.* **2021**, *420*, 129864.
[5] X. Wang, Y. Tang, S. Cheng, Q. Gao, Y. Yuan, A. Li, S. Guan, *Composites, Part A* **2022**, *161*, 107113.
[6] H. Cheng, Z. Lu, Q. Gao, Y. Zuo, X. Liu, Z. Guo, C. Liu, C. Shen, *Eng. Sci.* **2021**, *16*, 331.
[7] D. Guo, Y. Huo, C. Mu, B. Wang, J. Xiang, A. Nie, K. Zhai, T. Xue, F. Wen, Z. Liu, *J. Alloys Compd.* **2022**, *923*, 166401.
[8] Y. Jia, Y. Pan, C. Wang, C. Liu, C. Shen, C. Pan, Z. Guo, X. Liu, *Nano-Micro Lett.* **2021**, *13*, 201.
[9] J. Chen, J. Wu, H. Ge, D. Zhao, C. Liu, X. Hong, *Composites, Part A* **2016**, *82*, 141.
[10] D. Xing, L. Lu, Y. Xie, Y. Tang, K. S. Teh, *Mater. Des.* **2020**, *185*, 108227.
[11] S. Lin, S. Ju, J. Zhang, G. Shi, Y. He, D. Jiang, *RSC Adv.* **2019**, *9*, 1419.
[12] L.-C. Jia, C.-G. Zhou, W.-J. Sun, L. Xu, D.-X. Yan, Z.-M. Li, *Chem. Eng. J.* **2020**, *384*, 123368.
[13] J. Chang, H. Zhai, Z. Hu, J. Li, *Composites, Part B* **2022**, *246*, 110269.
[14] S. Zhang, X. Qi, M. Yang, Y. Cao, T. Lin, P. He, K.-W. Paik, *J. Mater. Sci.: Mater. Electron.* **2019**, *30*, 9171.
[15] T. Varol, O. Güler, S. B. Akçay, H. C. Aksa, *Powder Technol.* **2021**, *384*, 236.
[16] K. Zhang, X. Zhang, Q. Gao, M. Chan, S. Zhang, J. Li, W.-H. Liao, *Composites, Part A* **2023**, *167*, 107435.
[17] Y. Huang, Y. Wang, X. Sun, X. Guo, Y. Zhang, Z. Wang, P. Liu, C. Liu, J. Qiu, Y. Zhang, *Smart Mater. Struct.* **2020**, *29*, 045014.
[18] S.-S. Xue, Z.-H. Tang, W.-B. Zhu, Y.-Q. Li, P. Huang, S.-Y. Fu, *Compos. Commun.* **2022**, *29*, 100987.
[19] Y. Jung, J. Choi, W. Lee, J. S. Ko, I. Park, H. Cho, *Adv. Funct. Mater.* **2022**, *32*, 2201147.
[20] J. Wei, Z. Lin, Z. Lei, Y. Xu, Z. Zhao, T. Zhao, Y. Hu, H. Miao, R. Sun, *ACS Appl. Mater. Interfaces* **2022**, *14*, 5940.
[21] Y. Xu, Z. Lin, K. Rajavel, T. Zhao, P. Zhu, Y. Hu, R. Sun, C.-P. Wong, *Nano-Micro Lett.* **2021**, *14*, 29.
[22] J.-H. Cai, M.-L. Huang, X.-D. Chen, M. Wang, *Appl. Surf. Sci.* **2021**, *540*, 148364.
[23] J.-H. Cai, X.-H. Tang, X.-D. Chen, M. Wang, *Composites, Part A* **2021**, *140*, 106188.
[24] Y. Zhan, Y. Cheng, N. Yan, Y. Li, Y. Meng, C. Zhang, Z. Chen, H. Xia, *Chem. Eng. J.* **2021**, *417*, 129339.
[25] J.-H. Cai, J. Li, X.-D. Chen, M. Wang, *Chem. Eng. J.* **2020**, *393*, 124805.
[26] T. Shao, J. Wu, Y. Zhang, Y. Cheng, Z. Zuo, H. Lv, M. Ying, C. P. Wong, Z. Li, *Adv. Mater. Technol.* **2020**, *5*, 2000032.
[27] X. Chi, Y. Cai, L. Yan, Z. Heng, C. Zhou, H. Zou, M. Liang, *ACS Appl. Mater. Interfaces* **2023**, *15*, 15986.
[28] Q. Gao, Y. Pan, G. Zheng, C. Liu, C. Shen, X. Liu, *Adv. Compos. Hybrid Mater.* **2021**, *4*, 274.
[29] S.-H. Park, J. Hwang, G.-S. Park, J.-H. Ha, M. Zhang, D. Kim, D.-J. Yun, S. Lee, S. H. Lee, *Nat. Commun.* **2019**, *10*, 2537.
[30] H. Pang, L. Xu, D.-X. Yan, Z.-M. Li, *Prog. Polym. Sci.* **2014**, *39*, 1908.
[31] H.-Y. Wu, L.-C. Jia, D.-X. Yan, J.-F. Gao, X.-P. Zhang, P.-G. Ren, Z.-M. Li, *Compos. Sci. Technol.* **2018**, *156*, 87.
[32] Y.-J. Tan, J. Li, J.-H. Cai, X.-H. Tang, J.-H. Liu, Z.-Q. Hu, M. Wang, *Composites, Part B* **2019**, *177*, 107378.
[33] D. Yang, J.-R. Tao, Y. Yang, Q.-M. He, Y.-X. Weng, B. Fei, M. Wang, *Compos. Struct.* **2022**, *292*, 115668.
[34] D. Yuan, H. Guo, K. Ke, I. Manas-Zloczower, *Composites, Part A* **2020**, *132*, 105837.
[35] C. Jiao, Z. Deng, P. Min, J. Lai, Q. Gou, R. Gao, Z.-Z. Yu, H.-B. Zhang, *Carbon* **2022**, *198*, 179.
[36] B. Wei, L. Zhang, S. Yang, *Chem. Eng. J.* **2021**, *404*, 126437.
[37] J. Yang, Y. Chen, C. Liu, H. Wang, X. Yan, X. Chai, Z. Chen, Y. Xia, H. Gao, H. Zhang, X. Liao, *J. Mater. Res. Technol.* **2023**, *23*, 5115.
[38] M. Peng, F. Qin, *J. Appl. Phys.* **2021**, *130*, 225108.
[39] L. Bin, W. Na, Y. Yunfei, P. Fei, W. Changxian, W. Gang, X. Long, L. Wei, L. Jiurong, Z. Zhihui, *Adv. Funct. Mater.* **2022**, *33*, 2213357.
[40] G. Dan, H. Yingjie, M. Congpu, W. Bochong, X. Jianyong, N. Anmin, Z. Kun, X. Tianyu, W. Fusheng, L. Zhongyuan, *J. Alloys Compd.* **2022**, *923*, 166401.
[41] S.-T. Hsiao, C.-C. M. Ma, H.-W. Tien, W.-H. Liao, Y.-S. Wang, S.-M. Li, Y.-C. Huang, *Carbon* **2013**, *60*, 57.
[42] Y. Hu, X. Liu, L. Tian, T. Zhao, H. Wang, X. Liang, F. Zhou, P. Zhu, G. Li, R. Sun, C.-P. Wong, *ACS Appl. Mater. Interfaces* **2018**, *10*, 38493.
[43] L.-C. Jia, L. Xu, F. Ren, P.-G. Ren, D.-X. Yan, Z.-M. Li, *Carbon* **2019**, *144*, 101.
[44] K. Jin, J. Xing, X. Liu, Z. Jiang, S. Yang, X. Yang, J. Ma, *J. Mater. Chem. A* **2021**, *9*, 26999.

[45] X. Jin, J. Wang, L. Dai, X. Liu, L. Li, Y. Yang, Y. Cao, W. Wang, H. Wu, S. Guo, *Chem. Eng. J.* **2019**, *380*, 122475.
[46] T.-W. Lee, S.-E. Lee, Y. G. Jeong, *ACS Appl. Mater. Interfaces* **2016**, *8*, 13123.
[47] C. Lei, Y. Zhang, D. Liu, K. Wu, Q. Fu, *ACS Appl. Mater. Interfaces* **2020**, *12*, 26485.
[48] Q. Liu, Y. Zhang, Y. Liu, Z. Liu, B. Zhang, Q. Zhang, *J. Alloys Compd.* **2021**, *860*, 158151.
[49] J. Ma, K. Wang, M. Zhan, *RSC Adv.* **2015**, *5*, 65283.
[50] F. Mingshuai, C. Ru, L. Yongzhen, L. Rongkun, M. Yue, Z. Qingqing, R. Shuai, T. Ping, B. Yuezhen, *Compos. Commun.* **2022**, *35*, 101293.
[51] F. Shahzad, M. Alhabeb, C. B. Hatter, B. Anasori, S. Man Hong, C. M. Koo, Y. Gogotsi, *Science* **2016**, *353*, 1137.
[52] B. Shen, Y. Li, D. Yi, W. Zhai, X. Wei, W. Zheng, *Carbon* **2016**, *102*, 154.
[53] Y.-J. Wan, P.-L. Zhu, S.-H. Yu, R. Sun, C.-P. Wong, W.-H. Liao, *Small* **2018**, *14*, 1800534.
[54] Y. Wang, H.-K. Peng, T.-T. Li, B.-C. Shiu, H.-T. Ren, X. Zhang, C.-W. Lou, J.-H. Lin, *Chem. Eng. J.* **2021**, *412*, 128681.
[55] Y. Wang, H.-K. Peng, T.-T. Li, B.-C. Shiu, X. Zhang, C.-W. Lou, J.-H. Lin, *Prog. Org. Coat.* **2020**, *147*, 105861.
[56] S. Wu, M. Zou, Z. Li, D. Chen, H. Zhang, Y. Yuan, Y. Pei, A. Cao, *Small* **2018**, *14*, 1800634.
[57] D. Xing, L. Lu, K. S. Teh, Z. Wan, Y. Xie, Y. Tang, *Carbon* **2018**, *132*, 32.
[58] Y.-H. Yu, C.-C. M. Ma, C.-C. Teng, Y.-L. Huang, S.-H. Lee, I. Wang, M.-H. Wei, *Mater. Chem. Phys.* **2012**, *136*, 334.
[59] Y. Yuan, X. Sun, M. Yang, F. Xu, Z. Lin, X. Zhao, Y. Ding, J. Li, W. Yin, Q. Peng, X. He, Y. Li, *ACS Appl. Mater. Interfaces* **2017**, *9*, 21371.
[60] Q. Gao, X. Wang, D. W. Schubert, X. Liu, *Adv. Nanocompos.* **2024**, *1*, 52.